JOURNAL OF MATERIALS SCIENCE 40 (2005) 3395–3402

# Development of hybrid Mg/$Al_2O_3$ composites with improved properties using microwave assisted rapid sintering route

W. L. E. WONG, S. KARTHIK, M. GUPTA
*Department of Mechanical Engineering, National University of Singapore, 9 Engineering Drive 1, Singapore 117576*
*E-mail: mpegm@nus.edu.sg*

In the present study, hybrid magnesium based composites reinforced with an equivalent of 5 vol.% of micron and nano-sized $Al_2O_3$ particulates were synthesized using powder metallurgy technique incorporating an innovative microwave assisted rapid sintering technique. Microstructural characterization revealed near equiaxed grain morphology and the presence of minimal porosity in all the samples. Mechanical characterization studies revealed that the coupled addition of micron and nano-sized particulate reinforcements in magnesium matrix leads to a significant increase in hardness, elastic modulus, 0.2% yield strength, ultimate tensile strength and a decrease in ductility when compared to pure magnesium. Tensile testing results further revealed an increase in elastic modulus and ductility with no apparent change in the 0.2% yield strength and ultimate tensile strength of the hybrid composites upon the addition of nano-sized alumina particulates from 0.5 to 0.75 volume percent. With an increase in nano-sized alumina particulates from 0.75 to 1%, the overall mechanical properties of the hybrid composites were enhanced with an increase being observed in the elastic modulus, 0.2% yield strength and ductility of the composites. An attempt is made in this study to investigate the feasibility of the processing methodology and to study the effects of the addition of particulate reinforcements of different sizes on the microstructure, physical and mechanical properties of magnesium.


## 1. Introduction

The increasing demand for high performance materials in ever increasing challenging applications has led to intensive research on the development of new and novel composite materials. Magnesium is gaining importance as matrix material as its density is about 35% lower than aluminum and hence it has tremendous potential to replace aluminum in weight-critical applications [1–5]. In order to realize the best properties from the matrix and reinforcement, it is essential that processing methodology should be innovatively designed [1, 6]. Metal matrix composites are commonly manufactured either by solid-phase, liquid-phase or two-phase synthesis routes [1–3, 6]. Solid-phase processing routes remain favorable for the applications which require finer microstructural features and higher strength levels. Among the various solid-state processing techniques, powder metallurgy is commonly used for the synthesis of particulate reinforced composites. One of the most important steps in powder-based synthesis methods is that of sintering. Sintering assists in improving density, reducing porosity and development of metal-metal bond between metallic powder and metal-ceramic bonds between matrix and ceramic reinforcement [1, 7].

Sintering of metal based materials is usually carried out using induction or resistance heating [7–9]. Recently, a new method of sintering metal-based materials using microwaves has been proposed [10, 11]. In conventional sintering, the heat is transferred to the powder compact from the outside to inside whereas in microwave sintering, heat transfer takes place from inside to outside. As a result, core of compact is less dense in the case of conventional sintering while the surface remains less dense in the case of pure microwave sintering [12]. The rapid heating rate and lower sintering time, however, remains some of the most attractive features of microwave sintering as it assists in minimizing microstructural coarsening [10, 11]. Microwave assisted sintering used in this present study combines the features of conventional and microwave sintering and allows the sintering in both inside-to-outside and outside-to-inside direction. As a result of this feature, it can also be termed as 2-directional sintering.

A review of existing literature revealed that no attempt has been made so far to synthesize magnesium based composites using the powder-based method that include 2-directional microwave assisted hybrid

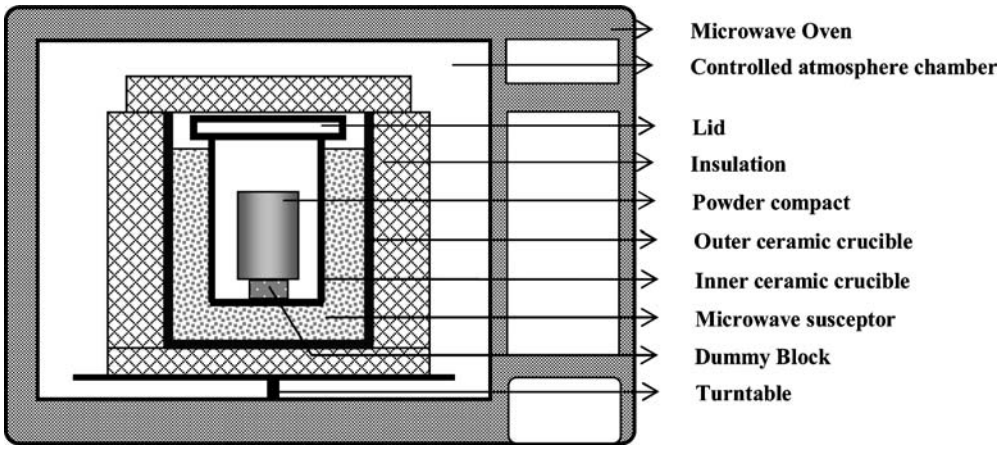


*Figure 1* Schematic diagram of experimental setup used in this study.

sintering involving radiant heat and microwaves under ambient atmospheric conditions. Literature survey also revealed that while various research attempts have been made to reinforce magnesium with one type of reinforcement such as ceramics [1–3, 13] or metallics [14–16], only limited studies have been conducted to reinforce magnesium with two types of reinforcements [17–19]. The synthesis approach used for hybrid composites so far, was liquid-based infiltration technique and the reinforcement length scale was in micrometer range. In all these attempts, researchers reported an improvement in tensile properties. Literature survey further revealed that no attempt is made to synthesize magnesium based composites using same type of reinforcement but with two different length scales, using powder approach and using rapid (2-directional) microwave-assisted hybrid sintering technique.

Accordingly, the aim of this study was to develop hybrid magnesium based composites utilizing microwave assisted 2-directional hybrid sintering approach. The sintered compacts were extruded and subsequently characterized in terms of physical, thermal and mechanical properties. Emphasis was placed to correlate the variation in properties with the relative amount of particulates of different length scales and at the same time to compare them with the properties of conventional Mg-based composites.

## 2. Experimental procedures

### 2.1. Materials

In this study, magnesium powder of 98.5% purity with a size range of 60–300 $\mu$m was used as the matrix material. Alumina powder of 0.3 $\mu$m and 50 nm in size were used as the reinforcements. The relative proportions of submicron and nano-sized $Al_2O_3$ were varied from 4 to 4.5% and 0.5 to 1% by volume, respectively. The overall volume fraction of reinforcements in all the formulations synthesized was fixed at 5 volume percent.

### 2.2. Processing

The hybrid magnesium matrix composites were synthesized using the powder metallurgy technique. The synthesis process involved blending pure magnesium powder with the submicron and nano-sized $Al_2O_3$ powder in a RETSCH PM-400 mechanical alloying machine at 200 rpm for 30 min. No balls or process control agent was used during blending step. The blended powder mixture was compacted at a pressure of 97 bar (50-tons) to billets (40-mm height, 35-mm diameter) using a 100-ton press. The compacted billets were sintered using an innovative hybrid microwave assisted 2-directional sintering technique. The billets were heated for 25 min to a temperature near the melting point of magnesium in a 900W, 2.45 GHz SHARP microwave oven. The schematic diagram of the experimental setup is shown in Fig. 1. The pure magnesium powder compact was compacted at the same pressure as the composite formulations and sintered for 25 min for benchmarking purpose.

The sintered billets of pure magnesium and its composite formulations were hot extruded at a temperature of 350°C with an extrusion ratio of 25:1 on a 150-ton hydraulic press using colloidal graphite as lubricant. The billets were soaked at 400°C for 1 h in a constant temperature furnace before extrusion. Final diameter of the rods obtained after extrusion was 7-mm.

### 2.3. Density measurements

The densities of the extruded samples were determined using Archimedes principle [20]. The samples were weighed in air and when immersed in distilled water using an A&D ER-182A electronic balance with an accuracy of $\pm$ 0.0001 g. Theoretical densities of the samples were calculated assuming they are fully-dense and there is no $Mg/Al_2O_3$ interfacial reaction.

### 2.4. Microstructural characterization

Microstructural characterization studies were conducted on polished specimens of pure magnesium and its composite formulations to investigate primarily the presence of porosity and morphological characteristics of the grains. The grain size and grain morphology were determined by image analysis of representative micrographs taken using an OLYMPUS metallographic

TABLE I Results of density and porosity measurements

| Materials | Reinforcement (vol.%) 50-nm | Reinforcement (vol.%) 0.3-$\mu$m | Theoretical density ($\rho$) (g/cm$^3$) | Experimental density ($\rho$) (g/cm$^3$) | Porosity (%) |
|---|---|---|---|---|---|
| Mg | – | – | 1.740 | $1.738 \pm 0.001$ | 0.07 |
| $Mg/Al_2O_3$ | 0.5 | 4.5 | 1.851 | $1.840 \pm 0.003$ | 0.58 |
| $Mg/Al_2O_3$ | 0.75 | 4.25 | 1.851 | $1.837 \pm 0.005$ | 0.75 |
| $Mg/ A1_2O_3$ | 1.0 | 4.0 | 1.851 | $1.831 \pm 0.005$ | 1.04 |

TABLE II Results of grain size study and CTE measurements

| Materials | Reinforcement (vol.%) 50-nm | Reinforcement (vol.%) 0.3-$\mu$m | Grain size ($\mu$m) | Aspect ratio | CTE $\times 10^{-6}/^{\circ}$C |
|---|---|---|---|---|---|
| Mg | – | – | $36 \pm 4$ | $1.68 \pm 0.45$ | $28.6 \pm 0.8$ |
| $Mg/Al_2O_3$ | 0.5 | 4.5 | $24 \pm 8$ | $2.26 \pm 0.91$ | $27.2 \pm 1.2$ |
| $Mg/Al_2O_3$ | 0.75 | 4.25 | $27 \pm 9$ | $1.83 \pm 0.51$ | $25.7 \pm 0.6$ |
| $Mg/Al_2O_3$ | 1.0 | 4.0 | $31 \pm 7$ | $1.65 \pm 0.42$ | $25.8 \pm 0.8$ |

microscope using the Scion Image Analyzer software. The microstructure of the samples was determined using JEOL JSM-5600LV scanning electron microscope.

### 2.5. Coefficient of thermal expansion

The coefficients of thermal expansion of extruded magnesium and hybrid composite formulations were determined using an automated SETARAM TMA 92–16.18 thermo-mechanical analyzer. Displacement of the samples as a function of temperature (50–400°C) was measured using an alumina probe under argon atmosphere. SETARAM software was used to determine the CTE values for the samples.

### 2.6. X-ray diffraction studies

X-ray diffraction analysis was carried out on the polished samples of extruded monolithic Mg and $Mg/Al_2O_3$ using an automated Shimadzu LAB-X XRD-6000 diffractometer. The samples were exposed to Cu $K_\alpha$ radiation ($\lambda = 1.54056$ Å) at a scanning speed of 2 deg/min. The Bragg angle and the values of the interplanar spacing (d) obtained were subsequently matched with the standard values for Mg, $Al_2O_3$ and related phases.

### 2.7. Mechanical behavior

Microhardness measurements were made on the polished samples of extruded monolithic Mg and $Mg/Al_2O_3$ hybrid formulations using a Matsuzawa MXT 50 automatic digital microhardness tester. The microhardness test was performed using a Vickers indenter under a test load of 25 gf and a dwell time of 15 s in accordance with the ASTM standard E3 84–99.

The tensile properties of the extruded Mg and hybrid composites were determined in accordance with ASTM standards E8M-01. The tensile tests were conducted on round tension test specimens of 5-mm in diameter and 25-mm gauge length using an automated servohydraulic testing machine (MTS 810) with a crosshead speed set at 0.254 mm/min. The tensile fractured specimens were investigated using scanning electron microscope to understand the fracture behavior of the monolithic and hybrid composite samples.

## 3. Results and discussion

### 3.1. Synthesis of Mg and $Mg/Al_2O_3$ hybrid composites

The synthesis of hybrid magnesium composites containing reinforcement of two different sizes was successfully achieved using two-directional microwave assisted sintering followed by hot extrusion. The results of macrostructural characterization on the extruded Mg and $Mg/Al_2O_3$ samples revealed the absence of macro defects. The outer surface was smooth and free of circumferential cracks. The results of density and porosity measurements indicate that near dense monolithic and composite formulations can be achieved using the fabrication methodology used in the present study (see Table I).

### 3.2. Microstructure

Microstructural characterization of the extruded Mg and $Mg/Al_2O_3$ composites revealed near equiaxed grain shape and the presence of submicron size $Al_2O_3$ at both intergranular and intragranular locations (see Fig. 2). Grain size analysis of the composite samples revealed a reduction in the average grain size of the matrix with the greatest reduction observed in samples containing the largest volume percent of submicron size $Al_2O_3$ (see Table II). The average grain size increased with a reduction in volume percentage of submicron size $Al_2O_3$ indicating a superior ability of submicron rather than nano-size $Al_2O_3$ particulates to inhibit grain growth. When compared to monolithic magnesium,

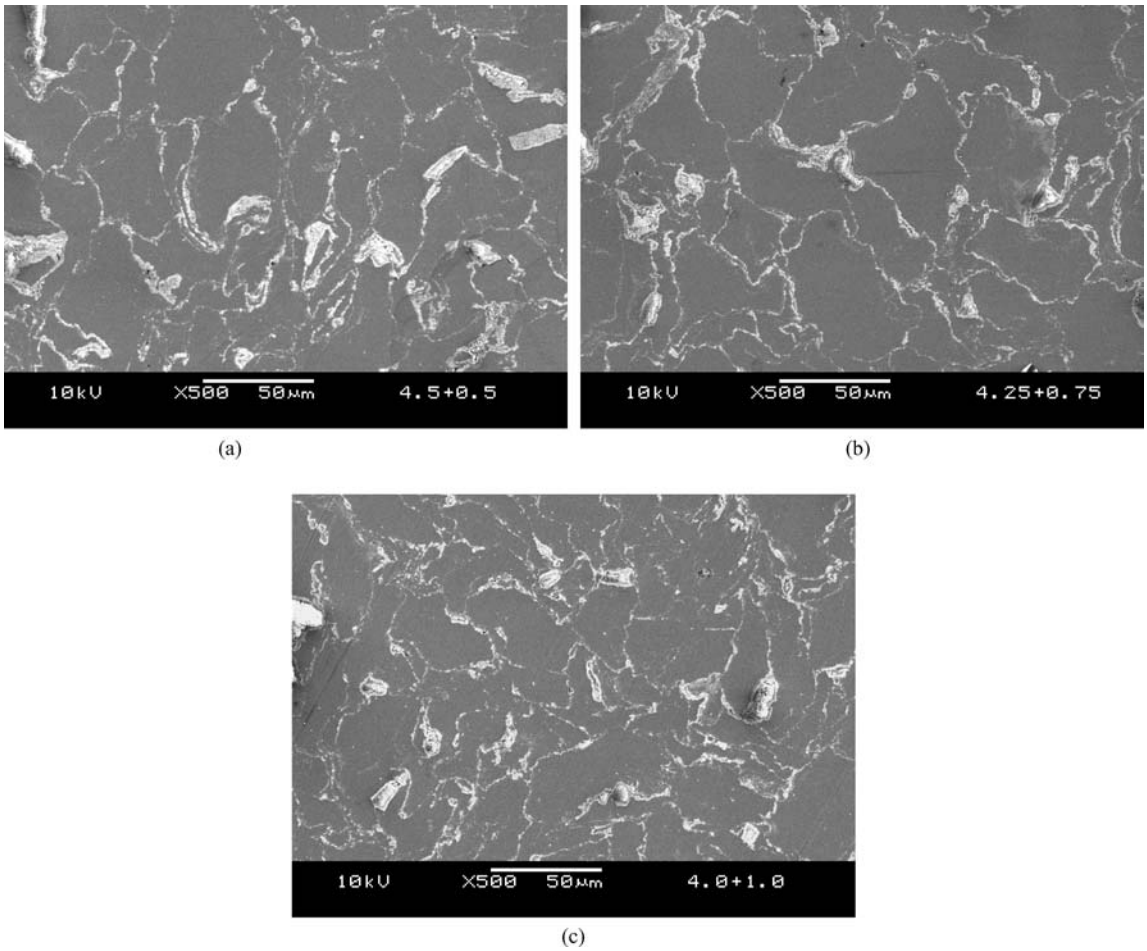


*Figure 2* Representative SEM micrographs showing the microstructures of: (a) Mg/4.5% (0.3-$\mu$m $A1_2O_3$)/0.5% (50-nm $A1_2O_3$), (b) Mg/4.25% (0.3-$\mu$m $A1_2O_3$)/0.75% (50-nm $A1_2O_3$), (c) Mg/ 4% (0.3-$\mu$m $A1_2O_3$)/1.0% (50-nm $A1_2O_3$).

the reduced grain size exhibited by the composite samples can primarily be attributed to the presence of reinforcement particulates and their ability to pin grain boundaries during sintering and hot extrusion steps.

### 3.3. Coefficient of thermal expansion

The results of CTE measurements in the temperature range of 50–400°C revealed that the coupled addition of submicron and nano sized $Al_2O_3$ reinforcements led to a reduction in the coefficient of thermal expansion values of the magnesium matrix (see Table II). The reduction in CTE values can be attributed to the presence of submicron and nano-$Al_2O_3$ reinforcements which exhibit a lower CTE value of 7.0 $\times$ $10^{-6}$/°C [1] when compared to pure magnesium (28.6 $\times$ $10^{-6}$/°C) and the ability of the reinforcements to effectively constraint the expansion of the matrix. Within the hybrid composites, the formulations containing 0.75–1% nano size $Al_2O_3$ appeared to give best results.

Theoretical CTE values were computed for the Mg/$Al_2O_3$ composite formulations using the Rule of Mixtures (upper bound, Equation 1), Turner's model (lower bound, Equation 2) and Kerner's model (Equation 3) [3] for comparison purposes using values provided in Table V. The equations can be represented as:

$$\alpha_{\text{comp}} = \alpha_m V_m + \alpha_r V_r \tag{1}$$

$$\alpha_{\text{comp}} = (\alpha_m V_m K_m + \alpha_r V_r K_r)/(V_m K_m + V_r K_r) \tag{2}$$

$$\alpha_{\text{comp}} = \alpha_m - V_r(\alpha_m - \alpha_r) \times \frac{K_m(3K_r + 4G_m)^2 + (K_r - K_m)\left(16G_m^2 + 12G_m K_r\right)}{(4G_m + 3K_r)[4V_r G_m(K_r - K_m) + 3K_r K_m + 4G_m K_m]} \tag{3}$$

where, $\alpha$, $V$, $K$, and $G$ represent coefficient of thermal expansion, volume fraction, bulk modulus and shear modulus of the phase while the subscript $m$ and $r$ refer to the matrix and reinforcement, respectively. The experimental and computed values of the coefficient of thermal expansion for the Mg/$Al_2O_3$ composite formulations are shown in Fig. 3. It is observed that: (i) the experimental values lie between the theoretical values predicted using Kerner's and Turner's models and (ii) the experimental CTE values are close to that predicted by Kerner's model for magnesium composite containing 0.5% nano-size $Al_2O_3$ and increasing volume percentage of nano-size $Al_2O_3$ particulates from 0.75 to 1.0% causes the CTE values to deviate further norther from the Kerner's model. In related studies, investigators reported that the CTE values of ZK60A magnesium

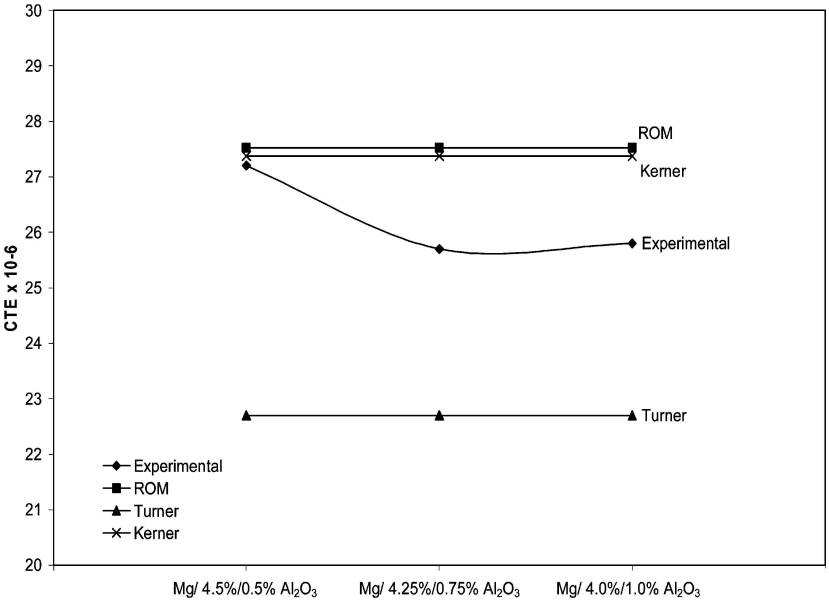


*Figure 3* Graphical representation showing the experimental and theoretical CTE values. Representative SEM micrographs taken from the tensile fracture surface of: (a) Pure Mg, (b) Mg/4.5% (0.3-$\mu$m $A1_2O_3$)/0.5% (50-nm $A1_2O_3$), (c) Mg/4.25% (0.3-$\mu$m $A1_2O_3$)/0.75% (50-nm $A1_2O_3$), (d) Mg/4% (0.3-$\mu$m $A1_2O_3$)/1.0% (50-nm $A1_2O_3$).

alloy reinforced with particulate SiC and particulate $B_4C$ reinforcements follow closely the Kerner's prediction [24]. The lower experimental values when compared to the Kerner's predictions indicates good realization of physical properties of the reinforcement and can be attributed to the coupled influence of: (i) reasonably uniform distribution of submicron and nano-sized $Al_2O_3$ particulates, and (ii) good interfacial integrity between $Al_2O_3$ particulates and the magnesium matrix. The significant deviation of CTE values of hybrid Mg-composites containing 0.75–1 vol% nano-$Al_2O_3$ from Kerner's prediction suggest the superior ability of $Al_2O_3$ in nano-length scale to control the dimensional stability of magnesium.

## 3.4. X-ray diffraction studies

The X-ray diffraction results corresponding to the Mg and hybrid Mg/$Al_2O_3$ samples were analyzed and the results of the phase analysis are shown in Table III.

## 3.5. Mechanical behavior

The results of microhardness measurements showed a marked increase in matrix hardness values in the case of hybrid magnesium composites (see Table III). The increase in microhardness can be attributed to the presence of relatively harder $Al_2O_3$ particulates as reinforcements, which acts as a constraint to localized matrix deformation during indentation and the reduction in grain size (see Table II). Amongst the hybrid composite formulations, the formulation with 0.75% nano-size $Al_2O_3$ exhibited the best microhardness value.

TABLE III Results of X-ray diffraction studies and microhardness measurements

| | Reinforcement (vol.%) | | No. of matching peaks | | |
|---|---|---|---|---|---|
| Materials | 50-nm | 0.3-$\mu$m | Mg | $A1_2O_3$ | Microhardness (HV) |
| Mg | – | – | 6[1] | – | 47.0 ±1.3 |
| Mg/$Al_2O_3$ | 0.5 | 4.5 | 6[1] | 4[1] | 56.6 ±1.2 |
| Mg/$A1_2O_3$ | 0.75 | 4.25 | 6[1] | 4[1] | 86.7 ±1.7 |
| Mg/$A1_2O_3$ | 1.0 | 4.0 | 6[1] | 4[1] | 73.7 ±1.1 |

[ ]represents the number of main peaks matched.

Tensile testing of the extruded specimens indicated an increase in elastic modulus, 0.2% yield strength and ultimate tensile strength of the hybrid composites and a reduction in ductility when compared to monolithic magnesium (see Table IV). Amongst the hybrid composites, the following trend was observed (see Table IV): (i) an increase in elastic modulus and ductility with no apparent change in the strength of the hybrid composites upon the addition of nano-size alumina particulates between 0.5 to 0.75 volume percent, (ii) with an increase in the nano-size alumina particulates from 0.75 to 1 volume percentage, the overall mechanical properties of the hybrid composites were enhanced with an increase being observed in the elastic modulus, 0.2% yield strength, UTS and ductility of the composites.

Elastic modulus measurements revealed that the coupled addition of submicron and nano-size $Al_2O_3$ leads to an increase in the elastic modulus of the magnesium matrix. The results further revealed that an increase in the relative proportion of nanosize $Al_2O_3$ particulates were more instrumental in increasing the elastic modulus of magnesium when compared to submicron size particulates (see Table IV). The results are consistent with the similar observation made on conventional Mg/$Al_2O_3$ nanocomposites [25]. The increase in elastic modulus of composite samples can be attributed to the presence of high modulus reinforcement ($E_{\text{alumina}} =$ 416 GPa [23]). Theoretical values for the elastic modulus were computed using the Rule of Mixtures [26] (Upper bound, Equation 4a), lower bound (Equation 4b) and Halpin-Tsai equation [1, 26] (Equation 5a and 5b)

TABLE IV Results of room temperature tensile properties

| Materials | Reinforcement (vol%) Submicron | Nano | Elastic modulus (GPa) | 0.2%YS (MPa) | UTS (MPa) | Ductility (%) |
|---|---|---|---|---|---|---|
| Mg | – | – | 45.0 | 116 ± 11.1 | 168 ± 10 | 9.0 ± 0.3 |
| $Mg/Al_2O_3$ | 4.5 | 0.5 | 50.5 | 139 ± 26.5 | 187 ± 28 | 1.9 ± 0.2 |
| $Mg/Al_2O_3$ | 4.25 | 0.75 | 51.9 | 138 ± 13.2 | 189 ± 15 | 2.4 ± 0.6 |
| $Mg/Al_2O_3$ | 4.0 | 1.0 | 54.4 | 157 ± 20.3 | 211 ± 21 | 3.0 ± 0.3 |
| Mg/ $SiC_p$[1] | 10 | – | 45 | 120 | 160 | 2 |
| AZ91/SiC[2] | 10 | – | 44.7 | 135 | 152 | 0.8 |
| Mg/21.3 SiC[3] | 21.3 | – | 50.0 | 128 ± 1.9 | 176 ± 3.5 | 1.4 ± 0.1 |
| $Mg/SiC/Al_2O_3{\cdot}SiO_2$[4] | 8 | – | 53.4 | – | 201.3 | 2.13 |

[1]Data obtained from reference 21.
[2]Data obtained from reference 2.
[3]Data obtained from reference 3.
[4]Data obtained from reference 18.

TABLE V Properties of magnesium and alumina

| Materials | CTE $\times 10^{-6}$ | Elastic modulus (GPa) | Bulk modulus (GPa) | Shear modulus (GPa) |
|---|---|---|---|---|
| Mg | 28.6[1] | 45[1] | 36[2] | 17.7[2] |
| $A1_2O_3$ | 7.0[3] | 416[4] | 257[4] | 169[4] |

[1]Data obtained from this study.
[2] Data obtained from Reference 22.
[3]Data obtained from Reference 1.
[4]Data obtained from Reference 23.

using the values provided in Table V:

$$E_c = V_m E_m + V_r E_r \tag{4a}$$

$$E_c = E_m\left[\frac{E_m V_m + E_r(V_r + 1)}{E_r V_m + E_m(V_r + 1)}\right] \tag{4b}$$

$$E_c = \frac{E_m(1 + 2sqV_r)}{1 - qV_r} \tag{5a}$$

$$q = \frac{E_r/E_m - 1}{E_r/E_m + 2s} \tag{5b}$$

where, $E$ represents elastic modulus, $s$ represents the aspect ratio of reinforcing phase and the subscripts $c$, $m$ and $r$ refer to the composite, matrix and reinforcement, respectively.

The experimental and theoretical values for the elastic modulus are shown in Fig. 4. The results show that the experimental values lie within the upper bound and Halpin-Tsai values. The experimental values remained superior when compared to Halpin-Tsai predictions indicating the superior ability of hybrid reinforcement to enhance elastic modulus when compared to the micron size reinforcement [3]. The experimental values obtained should still be considered lower-bound due to the presence of porosity. A model [27] was proposed recently that correlate the elastic modulus of the porous material ($E$) with the elastic modulus of the fully dense material ($E_0$) and the volume fraction of pores ($p$) through the following equations:

$$E = E_0(-p^{2/3})^{1{\cdot}21s} \tag{6a}$$

$$s = (z/x)^{1/3}\{1 + [(z/x)^{-2} - 1]\cos^2\alpha_d\}^{12} \tag{6b}$$

where $z/x$ is the aspect ratio of the pores and and $\alpha_d$ represents the relative orientation of the pores with respect to stress axis. The orientation factor $\cos^2\alpha_d$ is equivalent to 0.31 for a material with random orientation of pores which correspond to $\alpha_d$ of 56° [28]. Assuming $z/x = 1$, the corrected elastic modulus was computed and is shown in Fig. 4. The results indicate an upward correction indicating the achievable modulus from the hybrid composites synthesized in the present study.

The increase in 0.2%YS of the hybrid composites when compared to pure magnesium can be attributed to: (i) the Orowan strengthening mechanism triggered by nano-sized $Al_2O_3$ particulates, (ii) decrease in grain size, and (iii) increase in dislocation density around the particulates due to different thermal expansion behavior of the matrix and particulates. An improvement of ∼35% in 0.2%YS and ∼26% in UTS over that of pure magnesium was achieved with the addition of 4 vol% submicron and 1 vol% nano-size $Al_2O_3$ particulates. The addition of $Al_2O_3$ particulates led to a reduction in the ductility of the magnesium matrix. However, it was observed that within hybrid composites increasing addition of nano-size $Al_2O_3$ particulates led to an increase in ductility. The increase in ductility observed with increasing volume percentage of nano-size $Al_2O_3$ particulates in the case of magnesium is consistent with the findings reported elsewhere [13].

It may be noted that the overall combination of mechanical properties exhibited by hybrid composite formulations synthesized in this study is found to be superior when compared to conventional Mg-based composites containing higher volume fraction of reinforcement and synthesized using other processing routes [1–4] (see Table IV). This also establishes the feasibility of the microwave assisted 2-directional sintering technique used in this study to synthesize hybrid $Mg/Al_2O_3$ composite formulations with improved mechanical properties.

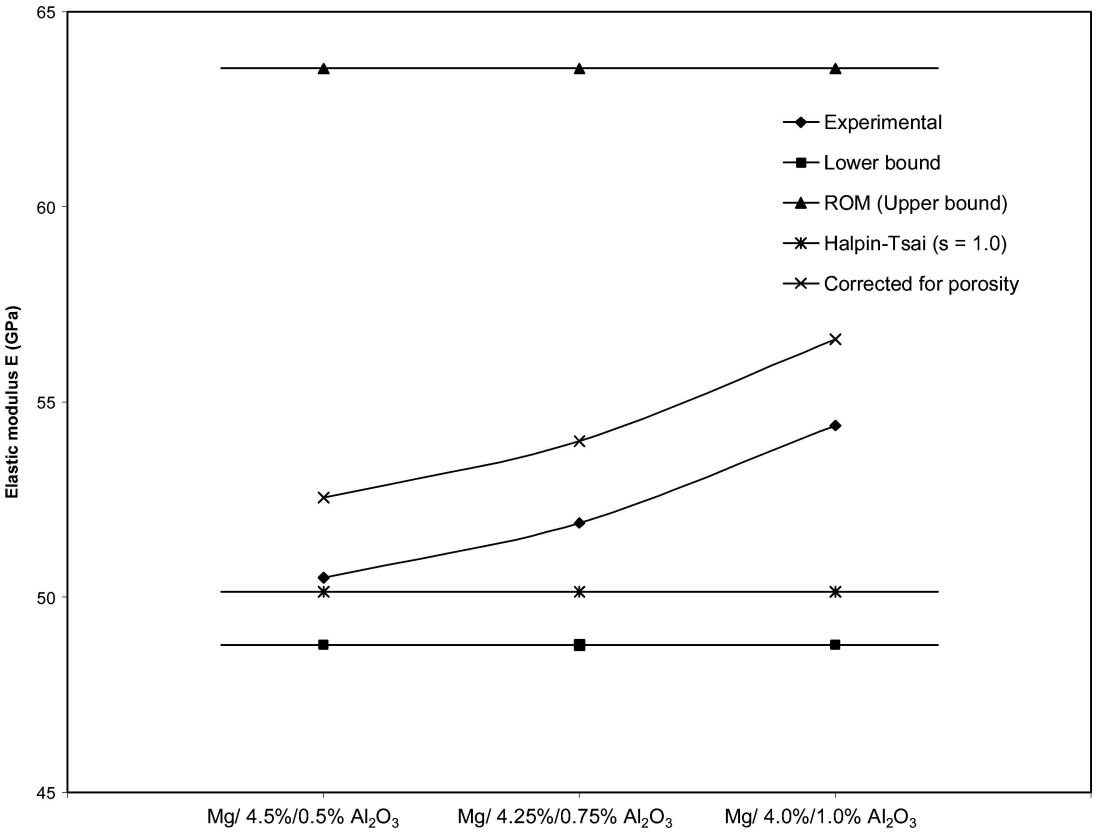


*Figure 4* Graphical representation showing the experimental and theoretical modulus values.

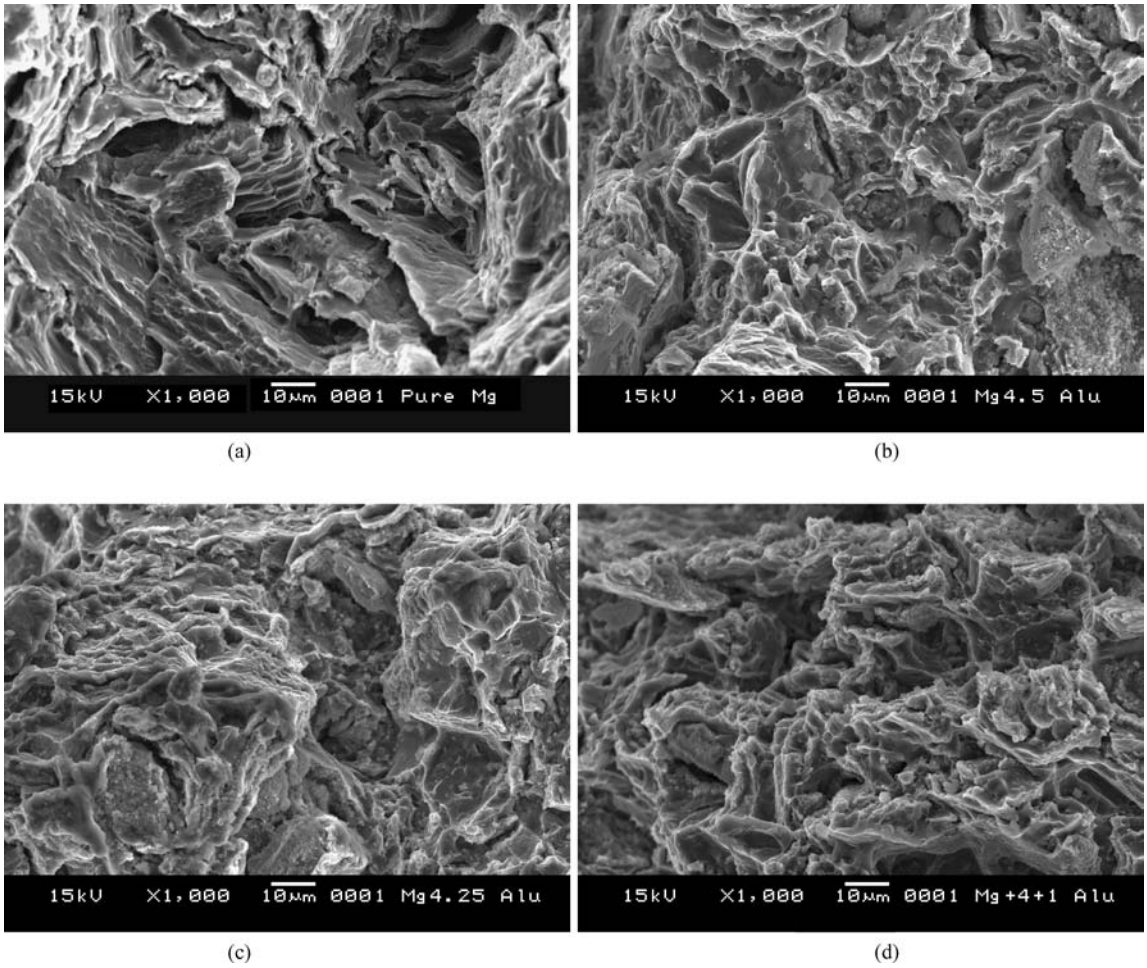


*Figure 5* Representative SEM micrographs taken from the tensile fracture surface of: (a) Pure Mg, (b) Mg/4.5% (0.3-$\mu$m $Al_2O_3$)/0.5% (50-nm $Al_2O_3$), (c) Mg/4.25% (0.3 $\mu$m $Al_2O_3$)/0.75% (50-nm $Al_2O_3$), (d) Mg/4% (0.3-$\mu$m $Al_2O_3$)/1.0% (50-nm $Al_2O_3$).

### 3.6. Fracture behavior

The results of fracture surface analysis revealed a typical brittle fracture in the case of Mg samples (see Fig. 5). This can be attributed to the HCP crystal structure of magnesium that restricts the slip to the basal plane. The presence of cleavage steps and microscopically rough fracture surface indicates the inability of magnesium to deform significantly under uniaxial tensile loading. For the hybrid composite formulations, the fracture surface revealed a predominantly brittle fracture with refined fracture features (see Fig. 5). This can be attributed to particle damage during tensile loading and subsequent initiation and propagation of cracks along different paths. In related studies [3], investigators have convincingly shown the ability of ceramic particulates such as SiC to crack the SiC/Mg interfacial region even in the absence of tensile loads. Further work is continuing in this area.

## 4. Conclusions

Following conclusions may be made from the results obtained in the present research investigation:

1. Powder metallurgy technique involving rapid microwave assisted 2-directional sintering and coupled with hot extrusion can be used to synthesize hybrid magnesium composites containing submicron and nano-$Al_2O_3$ particulates as reinforcements.

2. Results of coefficient of thermal expansion measurement indicate that the coupled addition of submicron and nano-$Al_2O_3$ reinforcements is able to improve the dimensional stability of magnesium matrix.

3. The coupled addition of submicron and nano-sized alumina reinforcements led to a significant increase in hardness, elastic modulus, yield strength and ultimate tensile strength but decreases the ductility of the composite formulations when compared to pure magnesium.

4. With an increase in the volume percent of nano-sized $Al_2O_3$ reinforcement from 0.75 to 1.0, the overall mechanical properties of the composites were enhanced with an increase being observed in elastic modulus, 0.2% yield strength, UTS and ductility of the composites.

## Acknowledgements

The authors wish to acknowledge with thank the financial support provided by NUS through research projects R-265-000-142-112 and R-265-000-169-112.

## References

1. D. J. LLYOD, *Int. Mater. Rev.* **39** (1994) 1.
2. A. LUO, *Metal. Mater. A* **26** (1995) 2445.
3. M. GUPTA, M. O. LAI and D. SARAVANARANGANTHAN, *J. Mater. Sci.* **35** (2000) 2155.
4. B. L. MORDIKE and K. U. KAINER, in "Magnesium Alloys and Their Applications" (Werkstoff-Insformations gesellschaft, Frankfu, Germany, 1998).
5. R. OAKLEY, R. F. COCHRANE and R. STEVENS, *Key. Eng. Mater.* **104** (1995) 387.
6. I. A. IBRAHIM, F. A. MOHAMED and E. J. LAVERNIA, *J. Mat. Sci.* **26** (1991) 1137.
7. R. M. GERMAN, in "Sintering Theory and Practice" (John Wiley & Sons Inc, New York, 1996) p. 2, 404.
8. R. M. GERMAN, in "Powder Metallurgy Science" (Metal Powder Industries Federation, USA, 1984).
9. J. P. SCHAFFER, A. SAXENA, S. D. ANTOLOVICH, T. H. SANDERS J. R. and S. B. WARNER, in "The Science and Design of Engineering Materials," 2nd ed. (McGraw Hill, 1999).
10. R. ROY, D. AGRAWAL, J. CHENG and S. GEDEVANISHVILI, *Nature* **399** (1999) 668.
11. D. AGRAWAL, *Mater. World* **7** (1999) 672.
12. R. ROY, J. CHENG, and D. K. AGRAWAL, US Patent No. 6,365,885 B1, April 2, 2002.
13. S. F. HASSAN and M. GUPTA, *Mat. Sci. Eng. A-Struct.* in press (2004).
14. S. F. HASSAN and M. GUPTA, *J. Alloy. Compd.* **345** (2002) 246.
15. S. F. HASSAN and M. GUPTA, *J. Alloy. Compd.* **335** (2002) L10.
16. S. F. HASSAN and M. GUPTA, *Mat. Res. Bull.* **37** (2002) 377.
17. J. SCHRÖDER and K. U. KAINER, *Mater. Sci. Eng. A-Struct* **135** (1991) 33.
18. X. N. ZHANG and R. J. WU, *Key. Eng. Mater.* **249** (2003) 217.
19. S. K. THAKUR, B. K. DHINDAW, N. HORT and K. U. KAINER, *Mater. Sci. Forum.* **426–432** (2003) 2027.
20. M. GUPTA, C. LANE and E. J. LAVERNIA, *Scr. Metall. Mater.* **26** (1992) 825.
21. M. R. KRISHNADEV, R. ANGERS, C. G. KRISHNADAS NAIR and G. J. HUARD, *J. Met.* **45** (1993) 52.
22. A. BUCH, in "Pure Metals Properties" (ASM International, Materials Park, Ohio, USA, 1999) p. 20.
23. Website: http://www.ceramics.nist.gov/srd/summary/scdaos.htm, last accessed Oct 2004.
24. A. L. GEIGER and M. JACKSON, *Adv. Mat. Proc.* **136**(7) (1989) 23.
25. S. F. HASSAN and M. GUPTA, *Mat. Sci. Tech.* in press (2004).
26. M. GUPTA and M. K. SURAPPA, *Key. Eng. Mat.* **104–107** (1995) 259.
27. A. R. BOCCACINI, G. ONDRACEK, P. MAZILU and D. WINDELBEG, *J. Mech. Behav. Mater.* **4** (1993) 11 9.
28. G. E. FOUGERE, L. RIESTER, M. FERBER, J. R. WEERTMAN and R. W. SIEGEL, *Mat. Sci. Eng. A—Struct* **204** (1995) 1.

*Received 5 November 2004*
*and accepted 4 January 2005*